Effective interactions between star polymers and colloidal particles

2001 J. Phys.: Condens. Matter 13 6177

(http://iopscience.iop.org/0953-8984/13/28/303)

INSTITUTE OF PHYSICS PUBLISHING JOURNAL OF PHYSICS: CONDENSED MATTER

J. Phys.: Condens. Matter **13** (2001) 6177–6194 PII: S0953-8984(01)25066-8

Effective interactions between star polymers and colloidal particles

A Jusufi, J Dzubiella, C N Likos, C von Ferber and H Löwen

Institut für Theoretische Physik II, Heinrich-Heine-Universität Düsseldorf, Universitätsstraße 1, D-40225 Düsseldorf, Germany

Received 21 May 2001
Published 29 June 2001
Online at stacks.iop.org/JPhysCM/13/6177

E-mail: jusufi@thphy.uni-duesseldorf.de

Abstract

Using monomer-resolved molecular dynamics simulations and theoretical arguments based on the radial dependence of the osmotic pressure in the interior of a star, we systematically investigate the effective interactions between hard, colloidal particles and star polymers in a good solvent. The relevant parameters are the size ratio q between the stars and the colloids, as well as the number of polymeric arms f (functionality) attached to the common centre of the star. By covering a wide range of q's ranging from zero (star against a flat wall) up to about 0.75, we establish analytical forms for the star–colloid interaction which are in excellent agreement with simulation results. A modified expression for the star–star interaction for low functionalities, $f \lesssim 10$ is also introduced.

1. Introduction

The study of the structural and thermodynamic properties of the polymeric state of matter has a long history in physics, which started with the pioneering work of Flory [1–3]. In the traditional 'polymeric approaches' to the matter, the chain nature of the macromolecules involved is at the forefront. However, in the last few years, alternative, complementary considerations have emerged that can loosely be called 'colloidal approaches'. Here, one envisions the polymer chains as diffuse, spherical objects and the chain nature of the molecules does not explicitly appear in the formalism. Instead, in a first step, almost all of the monomeric degrees of freedom are thermodynamically traced out of the problem [4]. Thereby, the polymers are replaced either by their centres of mass or by one of the monomers along their backbone, typically the end- or the central monomer. In this way, effective interactions between the polymers naturally arise [4], which implicitly include the effects of the traced-out monomers and typically have the range of the chain radius of gyration R_g. The earliest such approach dates back to the work of Asakura and Oosawa [5, 6], and Vrij [7], who modelled polymer chains as penetrable spheres. These models pertain mostly to Gaussian, i.e., ideal chains and are semi-quantitative.

0953-8984/01/286177+18$30.00

More systematic approaches have appeared in recent years, in which self-avoiding chains are modelled and effective interactions among them are derived by means of simulations [8] or theory [9]. The gain from adopting such an alternative view is twofold: on the one hand, one has the possiblity of looking at the same problem from a different angle; on the other hand, tracing out the monomers reduces the complexity of the problem by a factor N, the degree of polymerization of the chains [10].

A physical system where the colloidal approach finds an intuitive and natural application is that of star polymers [11]. These macromolecular entities are synthesized by covalently attaching f polymeric chains on a common centre. In this way, hybrid particles between polymers and colloids can be constructed, which naturally bridge the gap between these two common states of soft matter. The number of arms f, also known as *functionality* of the stars, allows us to go from free chains ($f = 1, 2$) to stiff, spherical particles ($f \gg 1$). Effective interactions between star polymers in good [12] and Θ-solvents [13] have been recently derived and the validity of the former has been confirmed through extensive comparisons with experiments [12, 14, 15] and simulations [16, 17]. Extensions to polydisperse stars [18] as well as to many-body forces in dense star polymer solutions [19] have also been recently carried out.

In this work, we wish to carry these considerations one step further by looking at a *two-component* system of star polymers in good solvent conditions and hard, spherical, colloidal particles. Though the star–star interaction is readily available and the colloids can be modelled as hard spheres, the effective cross interaction between star polymers and colloids is still missing. It is the purpose of this work to present theoretical and simulation results and to furnish analytic expressions for the force and/or the effective interaction acting between a star polymer and a spherical, colloidal particle for a large range of size ratios between the two. The theoretical approach is inspired by the eariler considerations of Pincus [20] regarding the force acting between a star and a flat wall but are made more precise here and they are also extended to include the effects of curvature. The rest of this paper is organized as follows: in section 2 we present the general theoretical approach, both for flat and curved surfaces and derive analytic expressions for the star–colloid force which includes a handful of undetermined parameters. In section 3 we compare those with the results of monomer-resolved molecular dynamics simulations and determine the free parameters in order to achieve agreement between theory and simulation results. In section 4 we present a modified version of the star–star potential which is valid for very low arm numbers, $f \lesssim 10$, and in section 5 we summarize and conclude.

2. Theory

Let us first define the system under consideration and its relevant parameters. We consider a collection of star polymers with functionality f and hard, spherical colloidal particles, the interaction between the latter species being modelled through the hard sphere (HS) potential. By considering two isolated members of each species, i.e., one star and one colloid, our goal is to derive the effective interaction between the two. The colloids have a radius R_c, which is a well-defined length scale.

The stars, on the other hand, are soft, hairy balls without a sharply defined boundary and this leads to some freedom in defining length scales characterizing their spatial extent. The experimentally measurable length scale that naturally arises from small-angle neutron- or x-ray-scattering experiments (SANS or SAXS) is the radius of gyration R_g of the stars and the associated diameter of gyration $\sigma_g = 2R_g$. For the theoretical investigations on the subject, however, another length scale turns out to be more convenient, namely the so called corona radius R_s of the star or the associated corona diameter $\sigma_s = 2R_s$. The corona radius arises naturally in the blob model for the conformation of isolated stars, introduced by Daoud and

Cotton [21]. According to the Daoud–Cotton picture, the bulk of the interior of a star in good solvent conditions (and for sufficiently long arm chains), consists of a region in which the monomer density profile $c(s)$ follows a power-law as a function of the distance s from the star centre, namely:

$$c(s) \sim a^{-3} \left(\frac{s}{a}\right)^{-4/3} \bar{v}^{-1/3} f^{2/3} \tag{1}$$

with the monomer length a, the excluded volume parameter v and the reduced excluded volume parameter $\bar{v} \equiv v/a^3$. Outside this scaling region, there exists a diffuse layer of almost freely fluctuating rest chains, in which the scaling behaviour of the monomer profile is no longer valid. We define the corona radius R_s of the star as the distance from the centre up to which the scaling behaviour of the monomer density given by equation (1) above holds true. In what follows, we define the *size ratio* q between the stars and the colloids as:

$$q \equiv \frac{R_g}{R_c}. \tag{2}$$

In addition, the interior of the star forms a semidilute polymer solution in which scaling theory [22] predicts that the osmotic pressure Π scales with the concentration c as $\Pi(c) \sim c^{9/4}$. Combining the latter with equation (1) above, we obtain for the radial dependence of the osmotic pressure of the star within the scaling regime the relation:

$$\Pi(s) \sim k_B T \, f^{3/2} s^{-3} \qquad (s \leqslant R_s). \tag{3}$$

No relation for the osmotic pressure $\Pi(s)$ for the diffuse region $s > R_s$ is known to date. It is indeed one of the central points of this work to introduce an accurate ansatz for the latter, one that will allow us also to derive closed formulas for the effective force between a star and a hard object. This is the subject we examine below.

2.1. A star polymer and a flat wall

We begin by examining the simplest case, in which a star centre is brought within a distance z from a hard, flat wall, as depicted in figure 1. Going back an idea put forward some ten years ago by Pincus [20], we can calculate the force $F_{sw}(z)$ acting between the polymer and the wall by integrating the normal component of the osmotic pressure $\Pi(s)$ along the area of contact between the star and the wall. In the geometry shown in figure 1, this takes the form:

$$F_{sw}(z) = 2\pi \int_{y=0}^{y=\infty} \Pi(s) \cos\vartheta \; y \mathrm{d}y. \tag{4}$$

Using $z = s \cos\vartheta$ and $y = z \tan\vartheta$ we can transform equation (4) into:

$$F_{sw}(z) = 2\pi z \int_{z}^{\infty} \Pi(s) \mathrm{d}s. \tag{5}$$

Equation (5) above implies immediately that, if the functional form for the force $F_{sw}(z)$ were to be known, then the corresponding functional form for the osmotic pressure $\Pi(z)$ could be obtained through:

$$\Pi(z) \propto -\frac{\mathrm{d}}{\mathrm{d}z} \left(\frac{F_{sw}(z)}{z}\right). \tag{6}$$

To this end, we now refer to known, exact results regarding the force acting between a flat wall and a *single, ideal chain* whose one end is held at a distance z from a flat wall [23]. There, it has been established that the force $F_{sw}^{(id)}(z)$ is given by the relation:

$$F_{sw}^{(id)}(z) = k_B T \frac{\partial}{\partial z} \ln\left[\mathrm{erf}\left(\frac{z}{L}\right)\right] \tag{7}$$

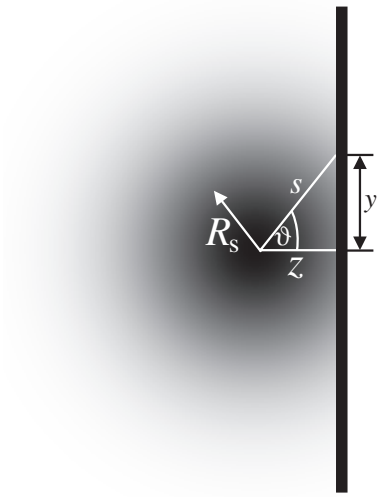

Figure 1. Star polymer (black-shadowed particle) interacting with a flat wall. The star polymer consists of a inner core region, where the scaling behaviour is dominant, whereas the outer regime is shadowed and indicates the exponential decay of the osmotic pressure.

where

$$\mathrm{erf}(x) = 2/\sqrt{\pi}\int_0^x e^{-t^2}\mathrm{d}t$$

denotes the error function and L is some length scale of the order of the radius of gyration of the polymer. Carrying out the derivative and setting $\mathrm{erf}(x) \cong 1$ for $x \gg 1$, we obtain a Gaussian form for the chain-wall force at large separations:

$$F_{\mathrm{sw}}^{(\mathrm{id})}(z) \cong \frac{k_B T}{L}\mathrm{e}^{-\frac{z^2}{L^2}} \qquad (z \gg L). \tag{8}$$

We now imagine a star composed of ideal chains. As the latter do not interact with each other ('ghost chains') the result of equation (8) holds for the star as well. Going now to self-avoiding chains, we assert that, as the main effect giving rise to the star-wall force is the volume which the wall excludes to the chains, rather than the excluded volume interactions between the chains themselves, a relation of the form (8) must also hold for the force $F_{\mathrm{sw}}(z)$ between a wall and a *real* star, but with the length scale L replaced by the radius of gyration or the corona radius of the latter and with an additional, f-dependent prefactor for taking into account the stretching effects of the f grafted polymeric chains. From equations (6) and (8) it now follows that

$$\Pi(s) \propto \frac{k_B T}{L}\left(\frac{1}{s^2} + \frac{2}{L^2}\right)\mathrm{e}^{-\frac{s^2}{L^2}} \qquad (s \gg L). \tag{9}$$

The full expression for $\Pi(s)$ now follows by combining equation (3), valid for $s \leqslant R_s$, with equation (9), valid for $s \gg L \cong R_s$, and matching them at $s = R_s$. The local osmotic pressure $\Pi(s)$ is the interior of a star polymer, as a function of the distance s from its centre has hence the functional form:

$$\Pi(s) = \Lambda f^{3/2} k_B T \begin{cases} s^{-3} & \text{for } s \leqslant R_s \\ \left(\dfrac{1}{s^2} + 2\kappa^2\right)\dfrac{\xi}{R_s}\mathrm{e}^{-\kappa^2(s^2 - R_s^2)} & \text{for } s > R_s \end{cases} \tag{10}$$

where Λ and $\kappa = L^{-1}$ are free parameters; it is to be expected that $\kappa = O(R_g^{-1})$, as we will verify shortly. On the other hand, ξ must be chosen to guarantee that $\Pi(s)$ is continuous at $s = R_s$, resulting in the value:

$$\xi = \frac{1}{1 + 2\kappa^2 R_s^2}. \tag{11}$$

Equation (10) above concerns the radial distribution of the osmotic pressure of an isolated star. The question therefore arises, whether this functional form for the osmotic pressure can also be used in order to calculate the force between a star and a flat wall in situations where the star-wall separation is smaller than the radius of gyration of the star, in which case it is intuitively expected that the presence of the wall will seriously disturb the monomer distribution around the centre and hence also the osmotic pressure. In fact, it is to be expected the osmotic pressure is a function of *both* the star-wall separation z and the radial distance s, whereas in what follows we are going to be using equation (5) together with equation (10), in which $\Pi(s)$ has no z-dependence itself. However, it turns out that this is an excellent approximation. On the one hand, it is physically plausible for large star-wall separations, where the presence of the wall has little effect on the segment density profile around the star centre and the ensuing osmotic pressure profile. On the other hand, also at very small star-wall separations, the scaling form $\Pi(s) \sim s^{-3}$ continues to be valid. To corroborate this claim, we proceed with some arguments to this effect.

First, we refer once more to known, exact results concerning the radial distribution of the pressure on a hard wall arising from an ideal chain grafted on it [24], a situation similar to holding one end of a chain at a distance very close to the wall surface. The pressure $\Pi_{\mathrm{id}}(s)$ reads as [24]:

$$\Pi_{\mathrm{id}}(s) = \frac{1}{2\pi}\frac{1}{(s^2+a^2)^{3/2}}\left(1+\frac{s^2+a^2}{2R_{\mathrm{g}}^2}\right)\exp\left[-\frac{s^2+a^2}{4R_{\mathrm{g}}^2}\right] \tag{12}$$

with the segment length a, indicating that in the regime $a \ll s \ll R_{\mathrm{g}}$ indeed the scaling $\Pi_{\mathrm{id}}(s) \sim s^{-3}$ holds.

Second, we can employ a scaling argument, asserting that, on dimensional grounds, the osmotic pressure exerted by a star on a nearby flat wall and held at a distance z from it, must be of the form $\Pi(s,z) = k_B T R_{\mathrm{g}}^{-3} h(s/R_{\mathrm{g}}, z/R_{\mathrm{g}})$, with some scaling function $h(x,y)$; universality arguments dictate that the segment length a should not appear in the dimensional analysis and hence s, z and R_{g} are the only relevant length scales for this problem. Now, for small star-wall separations, $z \ll R_{\mathrm{g}}$, we replace the second argument of this function by zero. Moreover, we assert that, as the dominant contribution to the osmotic pressure for distances $s < R_{\mathrm{g}}$ comes from the first few monomers along the chains colliding with the wall, the degree of polymerization N of the chains should be irrelevant if the chains are long. Hence, all R_{g}-dependence of the pressure should drop out, with the implication $h(x,0) \sim x^{-3}$ for $x \ll 1$ and hence $\Pi(s) \sim s^{-3}$ in this regime.

Third, we point out that bringing a star with f arms at a small distance to a flat wall, creates a conformation which is very similar to one of an isolated star with $2f$-arms, as shown in figure 2. Hence, it is not surprising that at small star-wall separations, one recovers for the radial dependence osmotic pressure the scaling laws pertinent to an isolated star.

Finally, by inserting equation (10) into equation (5) and carrying out the integration, we find that for small star-wall distances, $z \ll R_{\mathrm{s}}$, the force scales as $F_{\mathrm{sw}}(z) \sim (k_B T)/z$, thus giving rise to a logarithmic effective star-wall potential $V_{\mathrm{sw}}(z) \sim -k_B T \ln(z/R_{\mathrm{s}})$. The latter is indeed in full agreement with predictions from scaling arguments arising in polymer theory [20, 25, 26]. This is a universal result, in the sense that it also holds for single chains, be it real or ideal, as it can also be read off from the exact result, equation (7), using the property $\mathrm{erf}(x) \sim x$ for $x \to 0$. Thus, the proposed functional form for the osmotic pressure, equation (10), combined with equation (5) for the calculation of the effective force, has the following remarkable property: it yields the correct result both at small and at large star-wall distances and therefore appears to be a reliable analytical tool for the calculation of the effective force at *all* star-wall distances. At the same time, it contains two free parameters, Λ and κ

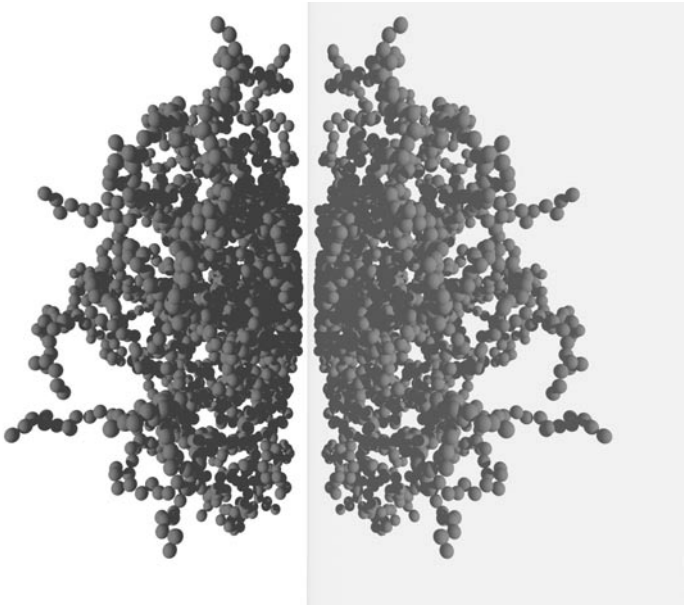

Figure 2. Snapshot of a simulation showing a star polymer interacting with a flat wall, at a small centre-to-surface distance. The mirror-reflected image of the star, on the right, helps demonstrate that the configuration is similar to that of an isolated star with twice as many arms.

which allow some fine tuning when the predictions of the theory are to be compared with simulation results, as we will do below. Yet, we emphasize that this freedom is *not* unlimited: on physical grounds, κ must be of the order of R_g^{-1} and Λ must be a number of order unity for all functionalities f, as the dominant, $f^{3/2}$-dependence of the osmotic pressure prefactor has been already explicitly taken into account in equation (10).

We are now in a position to write down the full expression for the star-wall force, by using equations (5) and (10). The result reads as:

$$\frac{R_s F_{sw}(z)}{k_B T} = \Lambda f^{3/2} \begin{cases} \dfrac{R_s}{z} + \dfrac{z}{R_s}(2\xi - 1) & \text{for } z \leqslant R_s \\ 2\xi \exp[-\kappa^2(z^2 - R_s^2)] & \text{for } z > R_s. \end{cases} \tag{13}$$

Note the dominant, $\sim 1/z$-dependence for $z \to 0$. Accordingly, the effective interaction potential $V_{sw}(z)$ between a star and a flat, hard wall held at a centre-to-surface distance z from each other reads as:

$$\beta V_{sw}(z) = \Lambda f^{3/2} \begin{cases} -\ln\left(\dfrac{z}{R_s}\right) - \left(\dfrac{z^2}{R_s^2} - 1\right)\left(\xi - \dfrac{1}{2}\right) + \zeta & \text{for } z \leqslant R_s \\ \zeta\, \mathrm{erfc}(\kappa z)/\mathrm{erfc}(\kappa R_s) & \text{for } z > R_s \end{cases} \tag{14}$$

with the inverse temperature $\beta = (k_B T)^{-1}$, the additional constant

$$\zeta = \frac{\sqrt{\pi}\xi}{\kappa R_s}\, \mathrm{erfc}(\kappa R_s)\, \mathrm{e}^{\kappa^2 R_s^2} \tag{15}$$

and the complementary error function $\mathrm{erfc}(x) = 1 - \mathrm{erf}(x)$. This completes our theoretical analysis of the star polymer–wall force and the ensuing effective interaction potential. The comparison with simulation data and the determination of the free parameters in the theory will be discussed in section 3. We now proceed with the calculation of the effective force between a star and a spherical hard particle, where effects of the colloid curvature become important.

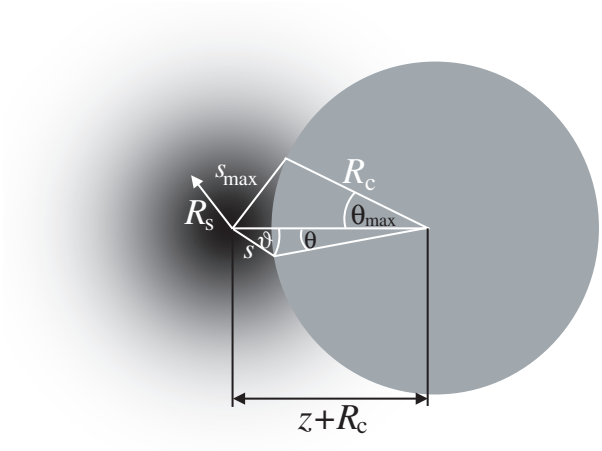

Figure 3. Star polymer (black-shadowed particle) interacting with a colloidal particle (grey sphere). The dark and shadowed regions of the star have the same meaning as in figure 1.

2.2. A star polymer and a spherical colloid

We apply the same idea as for the case of the hard wall: the effective force acting at the centre of the objects is obtained by integrating the osmotic pressure exerted by the polymer on the surface of the colloid. In figure 3, the geometrical situation is displayed: within the corona radius of the star polymer $R_s = \sigma_s/2$, the osmotic pressure is determined by scaling laws; the outer regime is shadowed and signifies the Gaussian decay of the osmotic pressure. At centre-to-surface distance z (centre-to-centre distance $r = z + R_c$), the integration of the osmotic pressure is carried out over the contact surface between star and colloid. Taking into account the symmetry of the problem, e.g., its independence of the azimuthal angle, we obtain the force $F_{sc}(z)$ between the star and the colloid as:

$$F_{sc}(z) = 2\pi R_c^2 \int_0^{\theta_{max}} d\theta \ \sin\theta \, \Pi(s) \cos\vartheta \tag{16}$$

where ϑ and θ are polar angles emanating from the centre of the star polymer and the colloid, respectively. The variables ϑ and θ can be eliminated in favour of the variable s, which denotes the distance between the centre of the star and an arbitrary point on the surface of the colloid. This elimination is achieved by taking into consideration the geometrical relations (see figure 3):

$$s \ \sin\vartheta = R_c \sin\theta \tag{17}$$

and

$$s \ \cos\vartheta + R_c \cos\theta = R_c + z. \tag{18}$$

Equations (16), (17) and (18) yield for the star–colloid effective force the transformed integral:

$$F_{sc}(z) = \frac{\pi R_c}{(z + R_c)^2} \int_z^{s_{max}} ds \left[(z + R_c)^2 - R_c^2 + s^2\right] \Pi(s). \tag{19}$$

The maximum integration distance, s_{max}, depends geometrically on θ_{max}, as well as on the distance z of the star polymer to the surface of the colloid and on R_c. The relation reads as

$$\begin{aligned} s_{max} &= \sqrt{[z + R_c(1 - \cos\theta_{max})]^2 + (R_c \sin\theta_{max})^2} \\ &= \frac{1}{q}\sqrt{\left[qz + R_g(1 - \cos\theta_{max})\right]^2 + (R_g \sin\theta_{max})^2}. \end{aligned} \tag{20}$$

By introducing equation (10) into equation (19), an analytic expression for the effective force follows, which reads as

$$\frac{F_{\rm sc}(z)}{k_{\rm B}T} = \frac{\Lambda f^{3/2} R_{\rm c}}{(z+R_{\rm c})^2} \begin{cases} \left[(z+R_{\rm c})^2 - R_{\rm c}^2\right]\left[\dfrac{1}{2z^2} - \dfrac{1}{2{R_{\rm s}}^2} + \Psi_1(R_{\rm s})\right] - \\ \qquad \ln(\dfrac{z}{R_{\rm s}}) + \Psi_2(R_{\rm s}) & \text{for } z \leqslant R_{\rm s}; \\ \left[(z+R_{\rm c})^2 - R_{\rm c}^2\right]\Psi_1(z) + \Psi_2(z) & \text{for } z > R_{\rm s}. \end{cases} \tag{21}$$

Here, the functions $\Psi_1(x)$ and $\Psi_2(x)$ are given by:

$$\Psi_1(x) = \frac{\xi}{R_{\rm s}} {\rm e}^{\kappa^2 R_{\rm s}^2} \left[\frac{1}{x}{\rm e}^{-\kappa^2 x^2} - \frac{1}{s_{\rm max}}{\rm e}^{-\kappa^2 s_{\rm max}^2}\right] \tag{22}$$

and

$$\Psi_2(x) = \frac{\xi}{R_{\rm s}} {\rm e}^{\kappa^2 R_{\rm s}^2} \left[\frac{\sqrt{\pi}}{\kappa}\left[{\rm erf}\,(\kappa s_{\rm max}) - {\rm erf}\,(\kappa x)\right] + x{\rm e}^{-\kappa^2 x^2} - s_{\rm max}{\rm e}^{-\kappa^2 s_{\rm max}^2}\right] \tag{23}$$

where ξ is given by equation (11). Note that, for small distances, both regimes of the osmotic pressure contribute to the integral, whereas for larger distances, $z > R_{\rm s}$, only the Gaussian decay does so. Due to the additional dependence of $s_{\rm max}$ on the distance z, [see equation (20)], an analytical expression for the effective potential $V_{\rm sc}(z)$, analogous to equation (14) for the flat-wall case, is not possible here.

Some remarks regarding $F_{\rm sc}(z)$ are necessary. First, for small separations z, the force scales as $F_{\rm sc}(z) \sim (k_B T)/z$, the same behaviour found for the flat-wall case. Once more, we obtain the universal result mentioned above, which has been shown to be also valid for an ideal chain whose one end is held at a distance z from the surface of a hard sphere. Indeed, for this case the force is given by the exact relation [27]:

$$F_{\rm sc}^{\rm (id)}(z) = k_B T \frac{\partial}{\partial z} \ln\left[1 - \left(\frac{R_{\rm c}}{z+R_{\rm c}}\right){\rm erfc}\left(\frac{z}{L}\right)\right] \tag{24}$$

with L being a length scale of order $R_{\rm g}$. equation (24) above, yields $F_{\rm sc}^{\rm (id)}(z) \sim (k_B T)/z$ for $z \to 0$.

Second, let us consider the limit of small size ratios $q = R_{\rm g}/R_{\rm c}$. As can be seen from equation (20), the upper integration limit $s_{\rm max}$ scales as $R_{\rm g}/q$, whereas the decay parameter κ is of the order $R_{\rm g}^{-1}$. Hence, $\kappa s_{\rm max} \sim q^{-1}$, with the implication that for small enough q's, the argument $\kappa s_{\rm max}$ in the error function and in the Gaussian in equations (22) and (23) can be replaced by infinity. As we will shortly see, this is an excellent approximation up to $q \lesssim 0.3$, as both ${\rm erf}\,(x)$ and $\exp(-x^2)$ approach their asymptotic values for $x \to \infty$ rapidly. Then, the implicit z-dependence of the force $F_{\rm sc}(z)$ through $s_{\rm max}$ drops out and a z-integration of the latter can be analytically carried out to obtain an effective star polymer–colloid potential $V_{\rm sc}^{\infty}(z)$ which reads as [28]:

$$\beta V_{\rm sc}^{\infty}(z) = \Lambda f^{3/2}\left(\frac{R_{\rm c}}{z+R_{\rm c}}\right) \begin{cases} -\ln\left(\dfrac{z}{R_{\rm s}}\right) - \left(\dfrac{z^2}{R_{\rm s}^2} - 1\right)\left(\xi - \dfrac{1}{2}\right) + \zeta & \text{for } z \leqslant R_{\rm s} \\ \zeta\,{\rm erfc}(\kappa z)/{\rm erfc}(\kappa R_{\rm s}) & \text{for } z > R_{\rm s} \end{cases} \tag{25}$$

with the constant ζ given by equation (15). Clearly, in the limit $R_{\rm c} \to \infty$ ($q \to 0$), corresponding to a flat wall, equation (25) reduces to the previously derived result, equation (14). It is a remarkable feature that all effects of curvature are taken into account by the simple geometrical prefactor $R_{\rm c}/(z+R_{\rm c})$, for sufficently small size ratios q. In this respect, the above result bears close similarity to the well-known Derjaguin approximation [29].

3. Simulation

3.1. The simulation model

In order to check the theoretical prediction of the forces at hard objects, we performed a monomer-resolved molecular dynamics (MD) simulation and calculated the mean force at the centre of the star polymer to compare the data with theory. The model is based on the ideas of simulation methods applied on linear polymers and on a single star [30,31]. The main features are as follows.

A purely repulsive and truncated Lennard–Jones potential acts between all Nf monomers at distances r:

$$V_{\mathrm{LJ}}(r) = \begin{cases} 4\epsilon\left[\left(\frac{\sigma_{\mathrm{LJ}}}{r}\right)^{12} - \left(\frac{\sigma_{\mathrm{LJ}}}{r}\right)^{6} + \frac{1}{4}\right] & \text{for } r \leqslant 2^{1/6}\sigma_{\mathrm{LJ}} \\ 0 & \text{for } r > 2^{1/6}\sigma_{\mathrm{LJ}}. \end{cases} \tag{26}$$

Here, σ_{LJ} is the microscopic length scale of the beads and ϵ sets the energy scale. In accordance with previous work [16], we have chosen $T = 1.2\epsilon/k_B$.

An attractive FENE (finite extensible nonlinear elastic) potential additionally acts between neighbouring monomers along a chain [30]:

$$V_{\mathrm{FENE}}(r) = \begin{cases} -15\epsilon\left(\frac{R_0}{\sigma_{\mathrm{LJ}}}\right)^2 \ln\left[1 - \left(\frac{r}{R_0}\right)^2\right] & \text{for } r \leqslant R_0 \\ \infty & \text{for } r > R_0. \end{cases} \tag{27}$$

This interaction diverges at $r = R_0$, which determines the maximal relative displacement of two neighbouring beads. The energy ϵ is the same as in equation (26), whereas for the length scale R_0 we have chosen the value $R_0 = 1.5\,\sigma_{\mathrm{LJ}}$.

To accommodate the polymer arms, a hard core with radius R_{d} is introduced at the centre of the star; its size depends on the arm number f. Accordingly, the interactions between the monomers and the central particle were introduced. All monomers had a repulsive interaction $V_{\mathrm{LJ}}^{p}(r)$ of the truncated and shifted Lennard–Jones type with the central particle,

$$V_{\mathrm{LJ}}^{p}(r) = \begin{cases} \infty & \text{for } r \leqslant R_{\mathrm{d}} \\ V_{\mathrm{LJ}}(r - R_{\mathrm{d}}) & \text{for } r > R_{\mathrm{d}} \end{cases} \tag{28}$$

whereas the innermost monomers in the chain had an additional attractive potential $V_{\mathrm{FENE}}^{p}(r)$ of the FENE type, namely

$$V_{\mathrm{FENE}}^{p}(r) = \begin{cases} \infty & \text{for } r \leqslant R_{\mathrm{d}} \\ V_{\mathrm{FENE}}(r - R_{\mathrm{d}}) & \text{for } r > R_{\mathrm{d}}. \end{cases} \tag{29}$$

Finally, all monomers interact with the colloid or with the wall by a hard potential. We note that exactly this simulation model was already used by Grest *et al* in their simulations of linear and star polymers in good solvent conditions [30,31].

The timestep is typically $\Delta t = 0.002t^*$ with $t^* = \sqrt{m\sigma_{\mathrm{LJ}}^2/\epsilon}$ being the associated time unit and m the monomer mass. After a long equilibration time (500 000 MD steps), the mean force at the core of the star whose centre is held at the position $\boldsymbol{R}$ and its dependence on the arm number f separations, is calculated as the expectation value over all instantaneous forces acting on the star core:

$$\boldsymbol{F}(\boldsymbol{R}) = \left\langle -\nabla_{\boldsymbol{R}}\left[\sum_{k=1}^{fN} V_{\mathrm{LJ}}^{p}(|\boldsymbol{r}_k - \boldsymbol{R}|) + \sum_{l=1}^{f} V_{\mathrm{FENE}}^{p}(|\boldsymbol{r}_l - \boldsymbol{R}|)\right]\right\rangle \tag{30}$$

where the first sum is carried over all fN monomers of the star and the second only over the f innermost monomers of its chains. The direct force between the central particle and the wall did not need to be considered, as the centre-to-surface distance was always kept at values where this force was vanishingly small. Note that choosing the origin of the coordinate system on the surface of the colloidal particle or wall, at the point of nearest separation between the star centre and this surface, and also the z-axis in the direction connecting this origin with the star centre, we immediately obtain $R \equiv |\boldsymbol{R}| = z$.

We have carried out simulations for a variety of arm numbers f and size ratios q, allowing us to make systematic predictions for the f- and q-dependencies of all theoretical parameters. In attempting to compare the simulation results with the theoretical predictions, one last obstacle must be removed: in theory, the fundamental length scale characterizing the star is the corona radius R_s. The latter, however, is not directly measurable in a simulation in which, instead, we can only assess the radius of gyration R_g. Yet, we have previously found that the ratio between the two remains fixed for all considered arm numbers f, having the value $R_s/R_g \simeq 0.66$ [16]. We now proceed with the presentation of our MD results.

3.2. Star–wall and star–colloid interactions

We consider at first a star polymer near a hard wall. The theoretical prediction of the effective interaction force is given in equation (13). First, we consider the limit of small separations, $z \to 0$, which allows us on the one hand to test the theoretical prediction $F_{sw}(z) \cong k_B T \Lambda f^{3/2}/z$ there and on the other hand to fix the value of the prefactor Λ, which is expected to have in general a weak f-dependence. For this prefactor, some semi-quantitative theoretical predictions already exist. For $f = 1, 2$ the prefactor may be calculated from the bulk and the ordinary surface critical exponents ν, γ and γ^o, γ_1^o of the n-vector model. For $n = 0$ this results in $\Lambda(f = 1) = (\gamma - \gamma_1^o)/\nu$ and $2^{3/2}\Lambda(f = 2) = (\gamma - \gamma^o)/\nu = 1/\nu$ [32,33]. Numerical values for the exponents are known from renormalization group theory and simulation [34,35] and yield $\Lambda(f = 1) \approx 0.83$ and $\Lambda(f = 2) \approx 0.60$. On the other hand, for very large functionalities, $f \gg 1$, one can make an analogy between a star at distance z from a wall and two star polymers whose centres are kept at distance $r = 2z$ from each other [20]. Indeed, for very large f, the conformations assumed by two stars brought close to each other is one in which the chains of each star retract to the half-space where the centre of the star lies, a situation very similar to the star–wall case. Then, one can make the approximation $F_{sw}(z) \cong F_{ss}(2z)$, where F_{ss} denotes the star–star force. For the latter, it is known [12] that it has the form:

$$F_{ss}(r) = \frac{5}{18} f^{3/2} \frac{1}{r} \qquad (r \to 0) \tag{31}$$

implying for the coefficient Λ the asymptotic behaviour:

$$\lim_{f \to \infty} \Lambda(f) \equiv \Lambda_\infty = \frac{5}{36} \cong 0.14. \tag{32}$$

Since there is no theory concerning the values of Λ in the intermediate regime of f, Λ is used as fit parameter. Its value can be obtained by plotting the inverse force $1/F_{sw}(z)$ against z for small separations z to the hard wall. The results are shown in figure 4. Looking first at the inset, we see that, as for the earlier case of star–star interactions [16], the reciprocal force curves do not go through the origin, as a result of the finite core size, R_d. Once this is subtracted, though, straight lines passing through the origin are obtained, verifying in this way the $1/z$-behaviour of the force and the associated logarithmic dependence of the effective potential at small separations. The values for $\Lambda(f)$ can be immediately read off from the slope of the curves and they are summarized in table 1. There and in figure 5 we see that Λ is indeed a decreasing function of f but the asymptotic value $\Lambda_\infty = 5/36$ is still not achieved at arm numbers as high as $f = 100$.

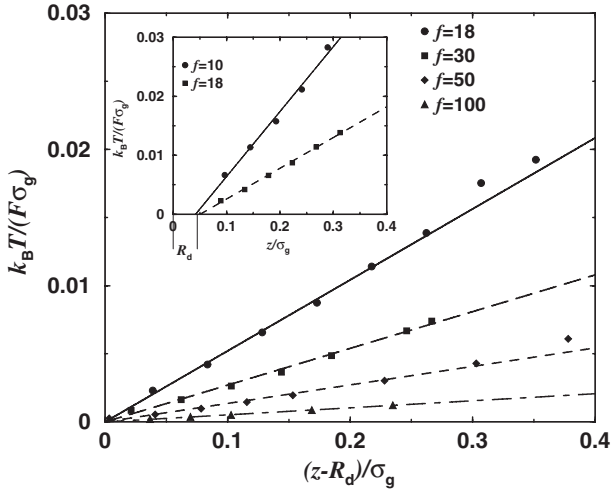

Figure 4. Reciprocal effective force between a star polymer and a hard flat wall plotted against the distance z between the star centre to the surface of the wall for small z-values. The dependence $F(z) \sim 1/z$ is confirmed by the simulation results (symbols). The prefactor of the potential depends on f and manifests itself in the different slopes of the reciprocal forces. The inset shows the divergence of the force at the distance $z = R_d$, which is subtracted from z in the outset of the plot, to achieve divergence of the force in the origin.

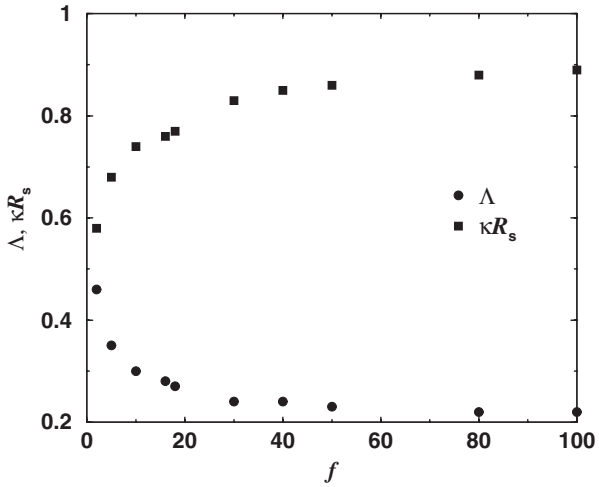

Figure 5. The prefactor of Λ and the decay parameter κ of equation (13) plotted against the functionality f. The value of $\Lambda = 5/36 \approx 0.14$ for $f \gg 1$ is not reached but the simulation data tend to this value very slowly. κ shows a monotonic increase with arm number f.

The decay parameter κ is fixed by looking at the force at larger separations and the obtained are also summarized in table 1 and shown in figure 5. As expected, κ is of the order R_g^{-1}, as witnessed by the fact that the product κR_s is of order unity. A monotonic increase of $\kappa\sigma_g$ with the arm number f is observed, consistent with the view that, for large f, stars form compact objects with an increasingly small diffuse layer beyond their coronae [12].

With parameters Λ and κ *once and for all fixed* from the star–wall case, we now turn our

Table 1. The fit parameters arising from the comparison between theory and simulation for the star–wall and star–colloid interaction. The values of R_d shown here are not exactly the same as the input core size; they are just in the same order of magnitude, deviating only slightly from the real input value. They are still corresponding to microscopic length, and are thus irrelevant at length scales $r \sim \sigma_s$. Λ is the overall prefactor and κ the inverse Gaussian decay length, both used in equations (21) and (25). $\sigma_s = 2R_s = 0.66\,\sigma_g$ denotes the corona diameter of the stars, as measured during the simulation.

f	R_d/R_s	Λ	κR_s
2	0.006	0.46	0.58
5	0.018	0.35	0.68
10	0.06	0.30	0.74
15	0.12	0.28	0.76
18	0.09	0.27	0.77
30	0.12	0.24	0.83
40	0.152	0.24	0.85
50	0.152	0.23	0.86
80	0.273	0.22	0.88
100	0.303	0.22	0.89

attention to the interaction of a star polymer at a hard sphere of finite radius R_c, equivalently size ratios $q \neq 0$. Here, the force is given by the full expressions of equations (21), (22) and (23); for small enough size ratios q, the approximation $\kappa s_{max} \to \infty$ gives rise to a simplified expression for the force and to the analytical formula, equation (25) for the effective star–colloid potential. Our purpose is twofold: to test the validity of these simplified expressions as a function of q and also to find an economical way to parameterize s_{max} as a function of q for those values of the size ratio for which the approximation $\kappa s_{max} \to \infty$ turns out to be unsatisfactory.

We show representative results for fixed arm number $f = 18$ and varying q in figure 6; results for different f-values are similar. It can be seen that the simplified result arising from allowing $s_{max} \to \infty$ yields excellent results up to size ratios $q \lesssim 0.3$, see Figs. 6(a) and (b). However, above this value, the approximation of integrating the osmotic pressure up to infinitely large distances breaks down, as it produces effective forces that are larger than the simulation results, especially at distances z of order of the radius of gyration R_g. These are the dashed lines shown in figures 6(c)–(e). The overestimation of the force is not surprising: as can be seen from figure 3 and equation (19), we are integrating a positive quantity beyond the physically allowed limits and this will inadvertently enhance the resulting force. Hence, we have to impose a finite upper limit s_{max} for size ratios $q > 0.3$ in order to truncate the contribution of the Gaussian tail in the integral of the osmotic pressure in equation (19).

In figure 7 a typical snapshot of a star polymer at a colloid illustrates the situation. One can see that the main contribution of the osmotic pressure results from the inner region of the star. The outer region of the chains only interact weakly with the sphere. The question now is how the value of s_{max} must be chosen. As can be seen from equation (20), this quantity is dependent on, R_s, z and θ_{max}. (The latter depending on q means that θ_{max} and q should not be treated as independent quantities.) It would indeed be most inconvenient if for every combination of these we had to choose a different upper integration limit. Hence, we have attempted to transfer all dependence of s_{max} onto the maximum integration angle θ_{max}. We found that this is indeed possible and, in fact, the angle $\theta_{max}(q)$ has a very weak q-dependence: starting with a value $\theta_{max} \approx 45^o$ at $q = 0.3$, we find that it then quickly saturates into the value $\theta_{max} \approx 30^o$ for all $q \gtrsim 0.35$. In this way, we are able to obtain the corrected curves denoted by the solid lines in figures 6(c)–(e), showing excellent agreement with the simulation results.

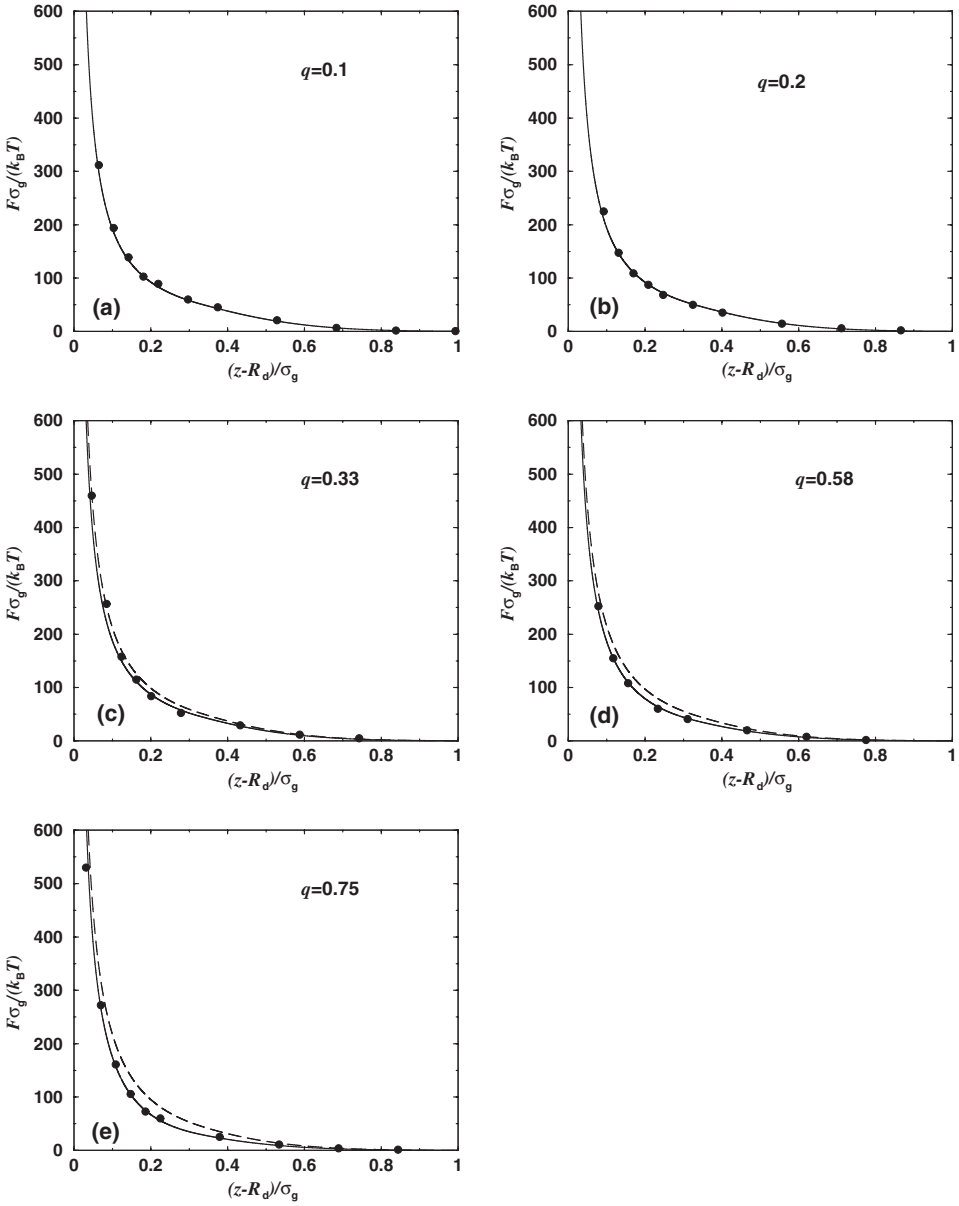

Figure 6. Comparison between simulation (symbols) and theoretical (lines) results for the effective force between a star polymer and a colloidal particle for different size ratios q, as a function of the centre-to-surface separation z. The arm number here is $f = 18$. The solid lines in (a) and (b) are derived from equation (21) for $s_{\max} \to \infty$. In (c)-(e) the dashed curves are derived by means of this approximation and they increasingly deviate from the simulation results as q grows. Thereby, a finite upper integration limit has to be introduced (see the text), producing the curves denoted by the solid lines in (c)–(e) and bringing about excellent agreement with simulation.

We finally turn our attention to the f-dependence of the forces for a fixed value of the size ratio, $q = 0.33$. In figure 8 we show the simulation results compared with theory for a wide range of arm numbers, $5 \leqslant f \leqslant 50$. For the theoretical fits, the values of Λ and κ from table 1

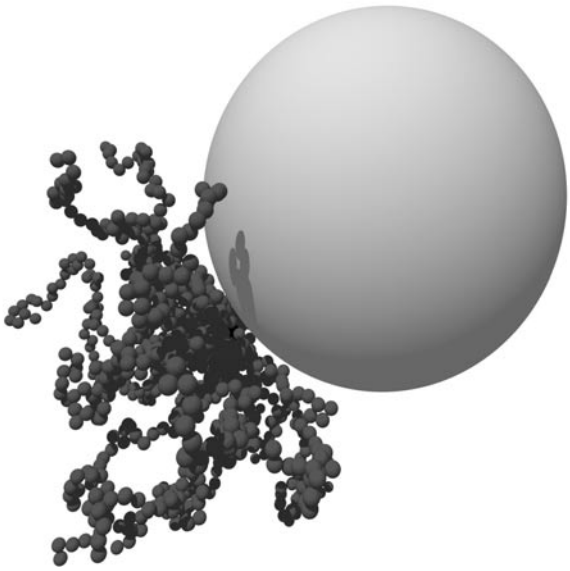

Figure 7. Snapshot of a typical configuration of a star polymer with $f = 18$ arms near a colloidal sphere with $q = 0.75$. One should notice that predominantly the inner region of the star interacts with the hard sphere, yielding the main contribution of the inner core regime to the osmotic pressure of a region, determined by $\theta_{\max} \approx 30^{\circ}$. Thereby, the upper integration limit $s_{\max}$ in equation (19) is limited, see also the geometrical aspects of equation (20) and figure 3.

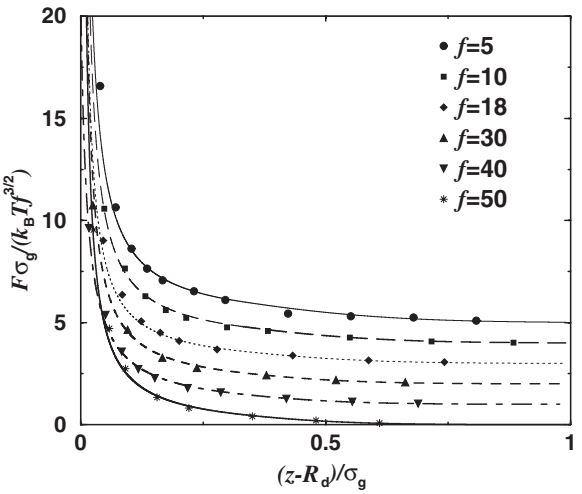

Figure 8. The effective force between a star polymer and a colloid for different arm numbers f and $q = 0.33$ plotted against z, the distance of the star centre to the surface of the colloid. The lines are the theoretical and the symbols the simulation results. For clarity, the data have been shifted upwards by constants: $f = 40 : 1$, $f = 30 : 2$, $f = 18 : 3$, $f = 10 : 4$, $f = 5 : 5$.

were used, whereas the value of the maximum integration angle was kept fixed at $\theta_{\max} = 30^{\circ}$ for all f-values. The agreement between theory and simulation is very satisfactory.

Thus, our conclusions for the star polymer–colloid interaction read as follows: the general,

analytical expression for the *force* between the two is given by equations (21), (22) and (23), supplemented by equation (20) in which the angle $\theta_{\max}$ has to be chosen as discussed above for $q \gtrsim 0.3$. An analytical formula for the effective *interaction potential* $V_{sc}(z)$ is not possible for such size ratios. Rather, the results for the effective force have to be integrated numerically in order to obtain $V_{sc}(z)$. For size ratios $q \lesssim 0.3$ on the other hand, the approximation $s_{\max} \to \infty$ in equations (21), (22) and (23) for the effective force can be made, thereby also allowing us to derive a simple, accurate, and analytic form for the interaction potential between a star polymer and a colloid, given by equation (25). These results form the basis of the statistical-mechanical treatment of star polymer–colloid mixtures in terms of standard liquid-state theories; the availability of analytical results for the pair interactions greatly facilitates the latter. A many-body theory of star polymer–colloid mixtures was put forward recently by Dzubiella *et al* [28], who employed the above-mentioned effective interactions in order to study the fluid-fluid separation (demixing transition) in such systems. The very good agreement with experimental results obtained in that work offers further corroboration of the validity of the interactions presented here.

As the ultimate goal of the derivation of the interactions we present here is precisely to allow theoretical investigations of star polymer–colloid mixtures, we present in the next section a short account of a revision of the star–star interactions for the case of very low arm numbers. In this way, mixtures containing stars with arbitrary arm numbers, ranging from free chains ($f = 1, 2$) to the 'colloidal limit' of $f \gg 1$ can be studied in full generality.

4. Revised star–star interaction for small arm numbers

The effective interaction between two stars in a good solvent was recently derived by theoretical scaling arguments and verified by neutron scattering and molecular simulation [12, 14–16], leading thereafter to the phase diagram of the system [36, 37]. The pair potential was modelled by an ultrasoft interaction which is logarithmic for an inner core and shows a Yukawa-type exponential decay at larger distances [12, 36]:

$$V_{ss}(r) = \frac{5}{18} k_B T f^{3/2} \begin{cases} -\ln\left(\dfrac{r}{\sigma_s}\right) + \dfrac{1}{1+\sqrt{f}/2} & \text{for } r \leqslant \sigma_s \\ \dfrac{\sigma_s/r}{1+\sqrt{f}/2} \exp\left(-\dfrac{\sqrt{f}}{2\sigma_s}(r-\sigma_s)\right) & \text{for } r > \sigma_s. \end{cases} \tag{33}$$

However, the theoretical approach giving rise to equation (33) does not hold for arm numbers $f \lesssim 10$, because the Daoud–Cotton model of a star [21], on which the Yukawa decay rests, is not valid for small f. In these cases, the interaction has to have a shorter-ranged decay for $r > \sigma_s$. The shortcomings of the blob model can be made evident if one considers the extreme limit $f = 1$, corresponding to free chains. There, the geometrical blob picture and the associated 'cone approximation' [38] break down. It is therefore instructive to consider known results about the effective interactions between free chains in order to obtain some insight for the case at hand.

Most of the work done on chain–chain interactions concerns the effective potential between the centres of mass of the chains [8, 10, 39–41]. Theoretical approaches considering two chains [41], simulations of two chains [39, 40], as well as recent, state-of-the-art simulations of many-chain systems [8, 10] all reach the conclusion that the effective centre-of-mass to centre-of-mass interaction has a Gaussian form with its range set by the radius of gyration of the chains. Here, we are interested in a slightly different interaction, namely that between the end-monomer of one chain and the end-monomer of the other. However, at distances of the order of R_g or larger, whether the centres of mass or the end-monomers choice of the two chains are held fixed should not make much difference. Therefore, we assume a Gaussian

decay of the star–star potential for small f-values and centre-to-centre distances larger than σ_s. We emphasize that *only* the large distance decay of the interaction is affected; its form at close approaches has to remain logarithmic [26]. Accordingly, we propose the following star–star pair potential for arm numbers $f < 10$, replacing the Yukawa by a Gaussian decay:

$$V_{ss}(r) = \frac{5}{18} k_B T f^{3/2} \begin{cases} -\ln\left(\dfrac{r}{\sigma_s}\right) + \dfrac{1}{2\tau^2\sigma_s^2} & \text{for } r \leqslant \sigma_s \\ \dfrac{1}{2\tau^2\sigma_s^2} \exp\left(-\tau^2(r^2 - \sigma_s^2)\right) & \text{for } r > \sigma_s \end{cases} \tag{34}$$

where $\tau(f)$ is a free parameter of the order of $1/R_g$ and is obtained by fitting to computer simulation results, see figure 9. For $f = 2$ we obtain the value $\tau = 1.03$ which, together with the potential in equation (34) above yields for the second virial coefficient of polymer solutions the value $B_2/R_g^3 = 5.59$, in agreement with the estimate $5.5 < B_2/R_g^3 < 5.9$ from renormalization group and simulations [10]. For $f = 5$ we find $\tau = 1.12$, which leads to $B_2/R_g^3 = 11.48$, in accordance with Monte Carlo simulation results [42, 43].

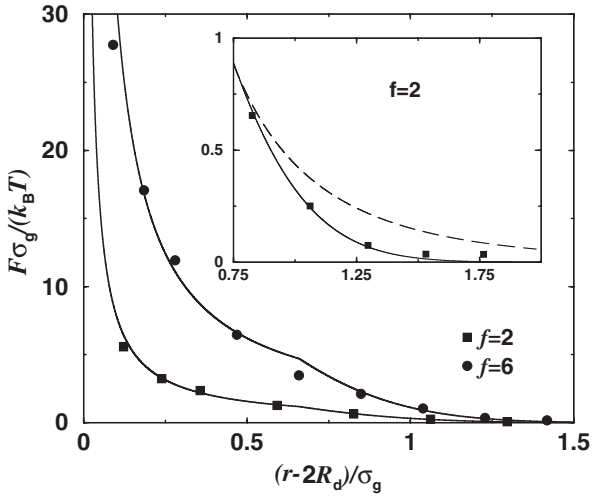

Figure 9. Effective force between two star polymers plotted against the centre-to-centre distance r for arm numbers $f = 2$ and $f = 6$. The simulation data (symbols) coincide with the logarithmic-Gauss expression (solid lines) of equation (34). In the inset, the outer distance region is enlarged in order to clearly show the validity of the Gaussian decay in this f-regime (solid line), whereas the Yukawa form (dashed line) produces poor agreement there.

The very good agreement between the logarithmic-Gauss-potential of equation (34) and the simulation data for $f < 10$ can be seen in figure 9. In the inset of this figure, it can also be seen that the Yukawa decay is far too slow there. Hence, the potential of equation (33), has a longer range than the true interaction for small f, a property that explains the discrepancies between the simulated and theoretical second virial coefficients based on this potential, which have been reported by Rubio and Freire [43] in their numerical study of low-functionality stars. At the same time, with increasing f, the roles of the Gaussian- and Yukawa-decays are reversed: in figure 10, we show simulation and theory results for $f = 10$. The original, logarithmic-Yukawa potential brings about better agreement now, as already established by earlier studies on stars with high arm numbers [12, 14, 16]. To summarize, we propose two analytic expressions for the effective star–star potential, valid in complementary regimes of the functionality f. The first one concerns the regime $f \lesssim 10$ with the validity of the

logarithmic-Gauss-potential of equation (34) being established; in the second regime, $f \geqslant 10$, the logarithmic-Yukawa-potential of equation (33) holds. We remark that the ultimative decay of the effective interaction for very long distances is still Gaussian even for very large f, but this is not relevant for B_2 as it occurs for much larger distances than the corona diameter.

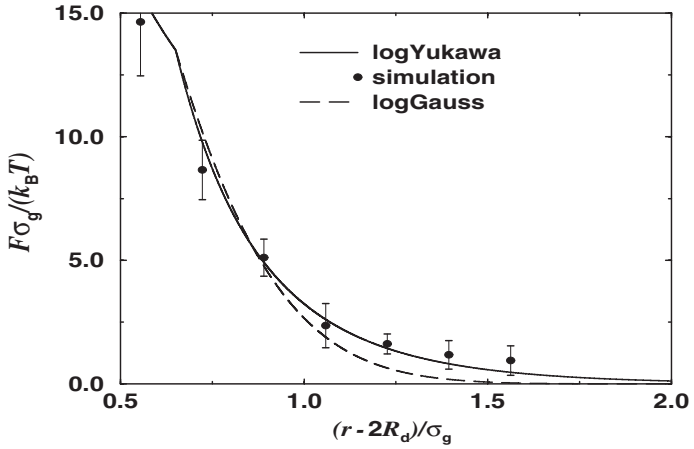

Figure 10. Effective force between two star polymers plotted against the centre-to-centre distance r for arm number $f = 10$. In contrast to figure 9, here the Yukawa form (solid line) gives an accurate description of the decay of the interaction at large separations, whereas the Gaussian form (dashed line) does not.

5. Summary and concluding remarks

In summary, we have presented analytic results for the force between a colloid and a star polymer in a good solvent, accompanied with an analytic expression for the corresponding pair potential which is valid for size ratios $q \lesssim 0.3$. The validity of these expressions was established by direct comparison with molecular dynamics simulations. It should be noted that our theoretical approach is in principle generalizable to arbitrary geometrical shapes for the hard particle, thus opening up the possibility for studying effective forces between stars and hard ellipsoids, platelets etc. Further, a revised form for the star–star interaction for small functionalities has been presented, while at the same time the logarithmic-Yukawa form of this interaction remains valid for functionalities $f \gtrsim 10$.

The practical advantage of the present results is that they greatly facilitate the study of structural and thermodynamic properties of concentrated star polymer–colloid mixtures; a first attempt towards this has already been undertaken [28]. In this work, we limited ourselves to the case where the star is smaller than the colloid, i.e., $q < 1$. The study of the inverse case may be possible by applying the ideas presented here, however additional complications arise through the possibility of the star to 'surround' the smaller, colloidal particle, in which case one part of the arms acts to bring about a repulsion with the colloid and another causes an effective attraction between the two. Furthermore, a pair potential picture for the many-body system becomes more and more questionable for larger q as effective many-body forces [19] will play a more dominant role in this case.

Acknowledgments

We thank E Eisenriegler and M Watzlawek for helpful discussions. This work has been supported by the Deutsche Forschungsgemeinschaft within the SFB 237.

References

[1] Flory P J 1942 *J. Chem. Phys.* **10** 51
[2] Flory P J 1949 *J. Chem. Phys.* **17** 303
[3] Flory P J 1953 *Principles of Polymer Chemistry* (Ithaca: Cornell University Press)
[4] Likos C N 2001 *Phys. Rep.* **348** 267
[5] Asakura S and Oosawa F 1954 *J. Chem. Phys.* **22** 1255
[6] Asakura S and Oosawa F 1958 *J. Polymer Sci.* **33** 183
[7] Vrij A 1976 *Pure Appl. Chem.* **48** 471
[8] Louis A A, Bolhuis P G, Hansen J-P, and Meier E J 2000 *Phys. Rev. Lett.* **85** 2522
[9] Fuchs M and Schweizer K S 2000 *Europhys. Lett.* **51** 621
[10] Bolhuis P G, Louis A A, Hansen J-P and Meier E J 2001 *J. Chem. Phys.* **114** 4296
[11] Grest G S, Fetters L J, Huang J S and Richter D 1996 *Adv. Chem. Phys.* **XCIV** 67
[12] Likos C N, Löwen H, Watzlawek M, Abbas B, Jucknischke O, Allgaier J and Richter D 1998 *Phys. Rev. Lett.* **80** 4450
[13] Likos C N, Löwen H, Poppe A, Willner L, Roovers J, Cubitt B and Richter D 1998 *Phys. Rev.* E **58** 6299
[14] Stellbrink J, Abbas B, Allgaier J, Monkenbusch M, Richter D, Likos C N, Löwen H and Watzlawek M 1998 *Progr. Coll. Polym. Sci.* **110** 25
[15] Stellbrink J, Allgaier J, Monkenbusch M, Richter D, Lang A, Likos C N, Watzlawek M, Löwen H Ehlers G and Schleger P 2000 *Progr. Coll. Polym. Sci.* **115** 88
[16] Jusufi A, Watzlawek M and Löwen H 1999 *Macromolecules* **32** 4470
[17] Shida K, Ohno K, Kimura M and Kawazoe Y 2000 *Macromolecules* **33** 7655
[18] von Ferber C, Jusufi A, Watzlawek M, Likos C N and Löwen H 2000 *Phys. Rev.* E **62** 6949
[19] von Ferber C, Jusufi A, Likos C N , Löwen H and Watzlawek M 2000 *Eur. Phys. J.* E **2** 311
[20] Pincus P 1991 *Macromolecules* **24** 2912
[21] Daoud M and Cotton J P 1982 *J. Physique* **43** 531
[22] de Gennes P G 1979 *Scaling Concepts in Polymer Physics* (Ithaca: Cornell University Press)
[23] Eisenriegler E 1993 *Polymers Near Surfaces* (Singapore: World Scientific)
[24] Bickel T, Marques C M, and Jeppesen C 2000 *Phys. Rev.* E **62** 1124
[25] Witten T A, Pincus P A and Cates M E 1986 *Europhys. Lett.* **2** 137
[26] Witten T A and Pincus P A 1986 *Macromolecules* **19** 2509
[27] Eisenriegler E 1997 *Phys. Rev.* E **55** 3116
[28] Dzubiella J, Jusufi A, Likos C N, von Ferber C, Löwen H, Stellbrink J, Allgaier J, Richter D, Schofield A B, Smith P A, Poon W C K and Pusey P N *Phys. Rev.* E **64** 010401(R)
[29] Hunter R J 1986 *Foundations of Colloid Science* vol I (Oxford: Clarendon)
[30] Grest G S, Kremer K and Witten T A 1987 *Macromolecules* **20** 1376
[31] Grest G S 1994 *Macromolecules* **27** 3493
[32] Dietrich S and Diehl H W 1981 *Z. Phys.* B **43** 315
[33] Ohno K and Binder K 1988 *J. Physique* **49** 1329
[34] Diehl H W and Shpot M 1998 *Nucl. Phys.* B **528** 595
[35] Hegger R and Grassberger P 1994 *J. Phys. A: Math. Gen.* **27** 4069
[36] Watzlawek M, Likos C N and Löwen H 1999 *Phys. Rev. Lett.* **82** 5289
[37] Watzlawek M, Löwen H, and Likos C N 1998 *J. Phys.: Condens. Matter* **10** 8189
[38] Ohno K 1989 *Phys. Rev.* A **40** 1524
[39] Grosberg A Y, Khalatur P G and A R Khokhlov 1982 *Makromol. Chem. Rapid Commun.* **3** 709
[40] Schäfer L and Baumgärtner A 1986 *J. Physique* **47** 1431
[41] Krüger B, Schäfer L and Baumgärtner A 1989 *J. Physique* **50** 3191
[42] Ohno K, Shida K, Kimura M and Kawazoe Y 1996 *Macromolecules* **29** 2269
[43] Rubio A M and Freire J J 2000 *Comp. Theor. Polymer Sci.* **10** 89